The *stum* Gene Is Essential for Mechanical Sensing in Proprioceptive Neurons

Bela S. Desai *et al.*

Science **343**, 1256 (2014);
DOI: 10.1126/science.1247761

Science (print ISSN 0036-8075; online ISSN 1095-9203) is published weekly, except the last week in December, by the American Association for the Advancement of Science, 1200 New York Avenue NW, Washington, DC 20005.

Together with the lineage analysis, these observations strongly suggest that the limb bud initiates earlier than stage 17 to 18, through EMT and independent of proliferation rate changes. When the limb bud mesenchyme is generated, it induces a source of fibroblast growth factor (Fgf) activity in the overlying ectoderm, the apical ectoderm ridge, which serves to maintain the limb's high level of proliferation (*3*). This does not occur in the trunk region, which we hypothesize is the reason for its relative decrease in mitotic activity as mesenchyme is generated. We suggest that the difference in proliferation of trunk versus limb bud mesenchyme is a result of limb bud initiation, as opposed to being a cause of it.

To verify that EMT of the somatopleure represents a necessary step of limb initiation, we blocked EMT in the presumptive limb region by RhoA overexpression, which abrogates EMT by inducing strong interaction of cells with extracellular matrix components (*4*). We electroporated RhoA with GFP within the epithelial somatopleure. In control embryos electroporated with GFP alone, limb buds formed normally (Fig. 2A), the basement membrane of laminin broke down, and cells underwent EMT (Fig. 2, B to D). In contrast, coelectroporation of RhoA with GFP completely abrogated limb formation (Fig. 2, E and I). Sections revealed that RhoA electroporated cells were stuck in the epithelial somatopleure and failed to undergo proper EMT (Fig. 2, F to H). These cells were attached to aggregates of laminin (Fig. 2, K and L) and did not exhibit enrichment in vimentin staining (fig. S5, G to L). We found that RhoA-overexpressing cells overexpressed F-actin, maintained adherens junction as revealed by N-cadherin and β-catenin stainings (fig. S5, A to L), and failed to relocalize aPKC from their apical cortex to the cytoplasm (fig. S5, A to F) as observed in control GFP-electroporated cells (fig. S4, N, O, R, and S). RhoA overexpression did not lead to dramatic reduction of proliferation (fig. S6, A to C) or increase in apoptosis in the electroporated cells (fig. S6, D to G), confirming that RhoA acts to prevent epithelial-to-mesenchymal cell state change. Thus as a consequence of this failure to undergo EMT, the electroporated cells did not participate in the initiation and formation of the limb primordium.

To understand how EMT is regulated in this context, we explored the possibility that Snail1, a transcription factor upstream of EMT in other contexts (*5*), plays a similar role here, but (perhaps because of redundancy) we failed to find such a connection. We therefore turned to factors known to be involved in establishing the formation of a limb bud. Ectopic Fgf protein, applied up to stage 17, is sufficient to induce the formation of an entire additional limb from trunk tissue (*6*). To test whether Fgf10 promotes limb formation by inducing EMT, we coelectroporated Fgf10 and GFP into the trunk somatopleure of stage-13 to -14 chick embryos. As expected, 36 hours after electroporation Fgf10 induced swelling of the trunk, indicating ectopic limb initiation (Fig. 3A, red arrowheads). Sectioning through the electroporated region showed that most of the GFP-positive cells had left the epithelium and had acquired a mesenchymal phenotype (81%, Fig. 3, B to D), showing that indeed EMT had taken place. The trunk is only competent to form an ectopic limb up to stage 16 to 17 (*7*, *8*). This was previously interpreted as the time at which the trunk mesenchyme becomes determined and is no longer capable of being redirected to a limb fate. However, our data show that this is precisely the time at which the trunk mesenchyme is first generated. Thus, we would reinterpret those results as indicating that ectopic Fgf activity can induce limb bud formation from epithelial trunk somatopleure cells but not from mesenchymal cells of the same rostrocaudal level.

Targeted mutation of Fgf10 and Tbx5 in mice have demonstrated that these genes are necessary to initiate limb bud formation (*9*–*12*). Transverse sections of embryonic day 9.5 *Fgf10*$^{-/-}$ and *Tbx5*$^{-/-}$ embryos confirmed that neither Tbx5 nor Fgf10 mutant embryos exhibit swellings characteristic of limb bud initiation (Fig. 3, E, H, and K). Both FGF10 and Tbx5 mutant embryos showed the presence of mesenchyme in the forelimb region; however, the proportion of mesenchymal cells compared to the proportion of epithelial cells was significantly lower than that of a wild-type (WT) sibling embryo (Fig. 3N), with a stronger phenotype observed in Tbx5$^{-/-}$ embryos (only 12% of cells were epithelial in WT embryos, whereas 21% and 51% were epithelial in Fgf10- and Tbx5-deficient embryos, respectively). In Tbx5 mutant embryos, the epithelium appeared separated from the mesenchyme (Fig. 3K, asterisks). aPKC and β-catenin staining revealed hyperplasia of the somatopleure epithelium, in support of failure of these cells to undergo EMT (Fig. 3, K and L). Last, in Fgf10$^{-/-}$ as well as in Tbx5$^{-/-}$ embryos, the basement membrane of laminin did not properly break down and appeared overstabilized, as opposed to WT embryos (Fig. 3, F, G, I, J, L, and M). Taken together, these data show that Tbx5 and Fgf10 act on the somatopleure epithelium to regulate, at least partially, the early induction of EMT in the limb fields, the process that is at the heart of limb bud initiation.

References and Notes

1. R. L. Searls, M. Y. Janners, *Dev. Biol.* **24**, 198–213 (1971).
2. A. Mauger, *J. Embryol. Exp. Morphol.* **28**, 313–341 (1972).
3. H. Ohuchi *et al.*, *Development* **124**, 2235–2244 (1997).
4. Y. Nakaya, E. W. Sukowati, Y. Wu, G. Sheng, *Nat. Cell Biol.* **10**, 765–775 (2008).
5. J. P. Thiery, H. Acloque, R. Y. J. Huang, M. A. Nieto, *Cell* **139**, 871–890 (2009).
6. M. J. Cohn, J. C. Izpisúa-Belmonte, H. Abud, J. K. Heath, C. Tickle, *Cell* **80**, 739–746 (1995).
7. H. Ohuchi *et al.*, *Biochem. Biophys. Res. Commun.* **209**, 809–816 (1995).
8. A. Vogel, C. Rodriguez, J. C. Izpisúa-Belmonte, *Development* **122**, 1737–1750 (1996).
9. P. Agarwal *et al.*, *Development* **130**, 623–633 (2003).
10. C. Rallis *et al.*, *Development* **130**, 2741–2751 (2003).
11. H. Min *et al.*, *Genes Dev.* **12**, 3156–3161 (1998).
12. K. Sekine *et al.*, *Nat. Genet.* **21**, 138–141 (1999).

Acknowledgments: We thank F. Constantini for help rederiving the Fgf10 mutant mouse line, B. Bruneau for kindly providing Tbx5 mutant embryos, and J. deMelo and P. Tschopp for help with mouse work. J.G. was a fellow of the Human Frontier Science Program. This work was supported by NIH grant R01-HD045499 to C.J.T.

Supplementary Materials

www.sciencemag.org/content/343/6176/1253/suppl/DC1
Materials and Methods
Supplementary Text
Figs. S1 to S6
Reference (*13*)

7 November 2013; accepted 7 February 2014
10.1126/science.1248228

The *stum* Gene Is Essential for Mechanical Sensing in Proprioceptive Neurons

Bela S. Desai, Abhishek Chadha, Boaz Cook*

Animal locomotion depends on proprioceptive feedback, which is generated by mechanosensory neurons. We performed a genetic screen for impaired walking in *Drosophila* and isolated a gene, *stumble* (*stum*). The Stum protein has orthologs in animals ranging from nematodes to mammals and is predicted to contain two transmembrane domains. Expression of the mouse orthologs of *stum* in mutant flies rescued their phenotype, which demonstrates functional conservation. Dendrites of *stum*-expressing neurons in legs were stretched by both flexion and extension of corresponding joints. Joint angles that induced dendritic stretching also elicited elevation of cellular Ca^{2+} levels—not seen in *stum* mutants. Thus, we have identified an evolutionarily conserved gene, *stum*, which is required for transduction of mechanical stimuli in a specific subpopulation of *Drosophila* proprioceptive neurons that sense joint angles.

Animal locomotion is achieved by coordination of motor activity according to proprioceptive mechanosensory inputs. In *Drosophila*, mechanosensation is mediated either by ciliated or multidendritic receptor neurons. Multidendritic neurons can respond to direct

application of mechanical force to their membranes (*1*, *2*). It is less clear, however, how multidendritic mechanosensory neurons can be tuned to one mechanical modality, such as joint angle, and disregard other mechanical stimuli that may originate from external impacts or changes in the shape of muscles during contraction. In order to identify genes involved in proprioceptive sensation, we screened for uncoordination in a collection of ethyl methanesulfonate–mutagenized *Drosophila* lines (*3*). Lines that exhibited walking impairments were selected, and the phenotype severity was quantified by measuring climbing speed. We identified three lines, 204, 922, and 4487, that showed lack of coordination in homozygous flies and did not complement one another (Fig. 1A), which suggested that they represent alleles of the same gene. Two of the lines, 204 and 4487, showed severe uncoordination, and the phenotype in 922 was mild (Fig. 1A). Deficiency mapping pointed to a gene, *CG30263* (Fig. 1B), predicted to encode a large protein with 1870 or 1959 amino acids (depending on the splice variant). Because the mutants had a walking impairment phenotype, we named this gene *stumble* (*stum*). The *stum* ortholog in humans is *C1orf95*, and it was categorized as a member of the SPEC3 family (UNIPROT, INTERPRO), with unknown function. We sequenced the *stum* gene in the three mutant lines and found that $stum^{204}$, $stum^{4487}$, and $stum^{922}$ had stop codons at amino acid positions 171, 202, and 1081, respectively (Fig. 1C).

We generated transgenic flies that express *stum* cDNA in neurons and found that the *stum*

Department of Molecular and Cellular Neuroscience, The Scripps Research Institute, La Jolla, CA 92037, USA.
*Corresponding author. E-mail: bcook@scripps.edu

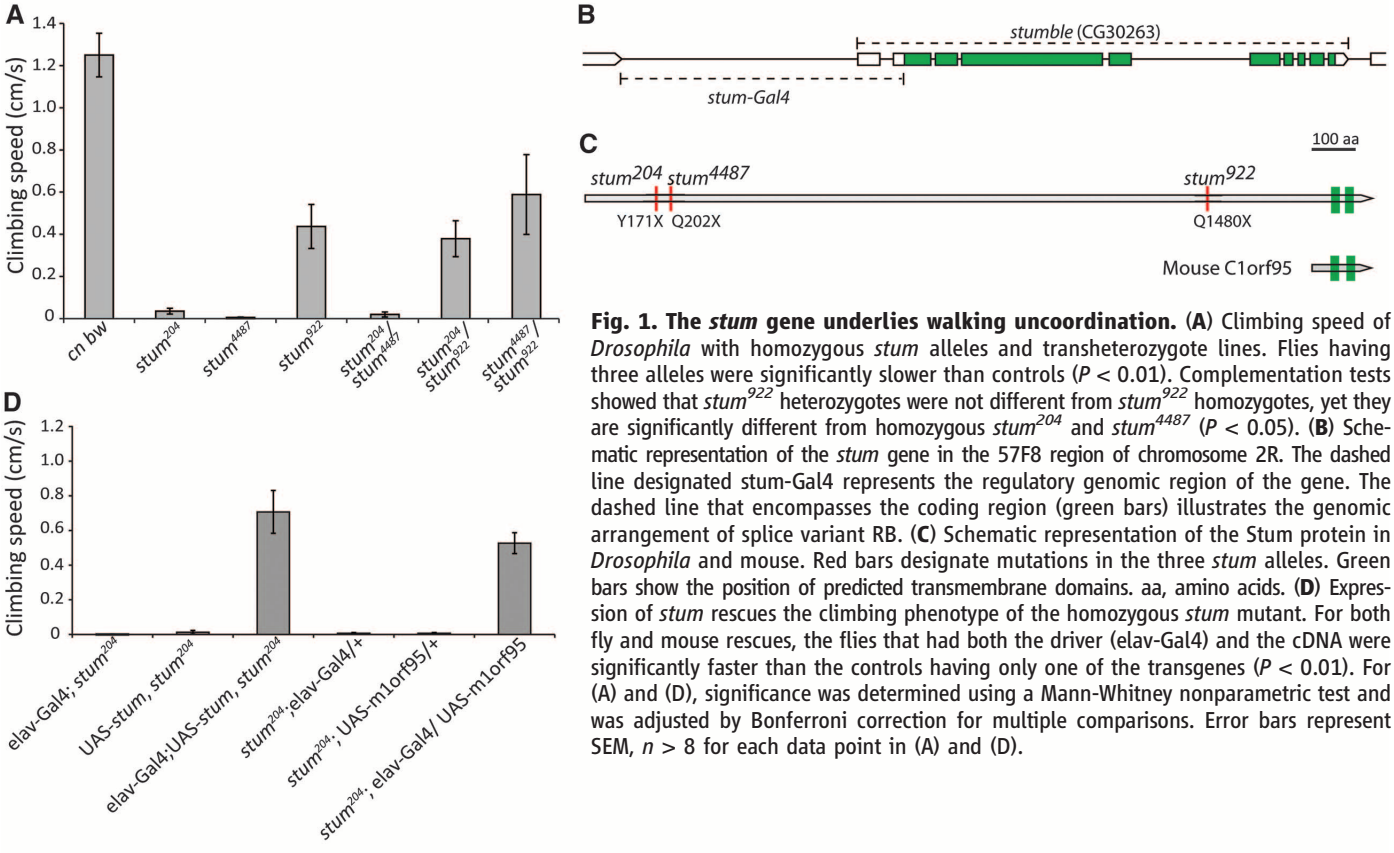

Fig. 1. The *stum* gene underlies walking uncoordination. (**A**) Climbing speed of *Drosophila* with homozygous *stum* alleles and transheterozygote lines. Flies having three alleles were significantly slower than controls ($P < 0.01$). Complementation tests showed that $stum^{922}$ heterozygotes were not different from $stum^{922}$ homozygotes, yet they are significantly different from homozygous $stum^{204}$ and $stum^{4487}$ ($P < 0.05$). (**B**) Schematic representation of the *stum* gene in the 57F8 region of chromosome 2R. The dashed line designated stum-Gal4 represents the regulatory genomic region of the gene. The dashed line that encompasses the coding region (green bars) illustrates the genomic arrangement of splice variant RB. (**C**) Schematic representation of the Stum protein in *Drosophila* and mouse. Red bars designate mutations in the three *stum* alleles. Green bars show the position of predicted transmembrane domains. aa, amino acids. (**D**) Expression of *stum* rescues the climbing phenotype of the homozygous *stum* mutant. For both fly and mouse rescues, the flies that had both the driver (elav-Gal4) and the cDNA were significantly faster than the controls having only one of the transgenes ($P < 0.01$). For (A) and (D), significance was determined using a Mann-Whitney nonparametric test and was adjusted by Bonferroni correction for multiple comparisons. Error bars represent SEM, $n > 8$ for each data point in (A) and (D).

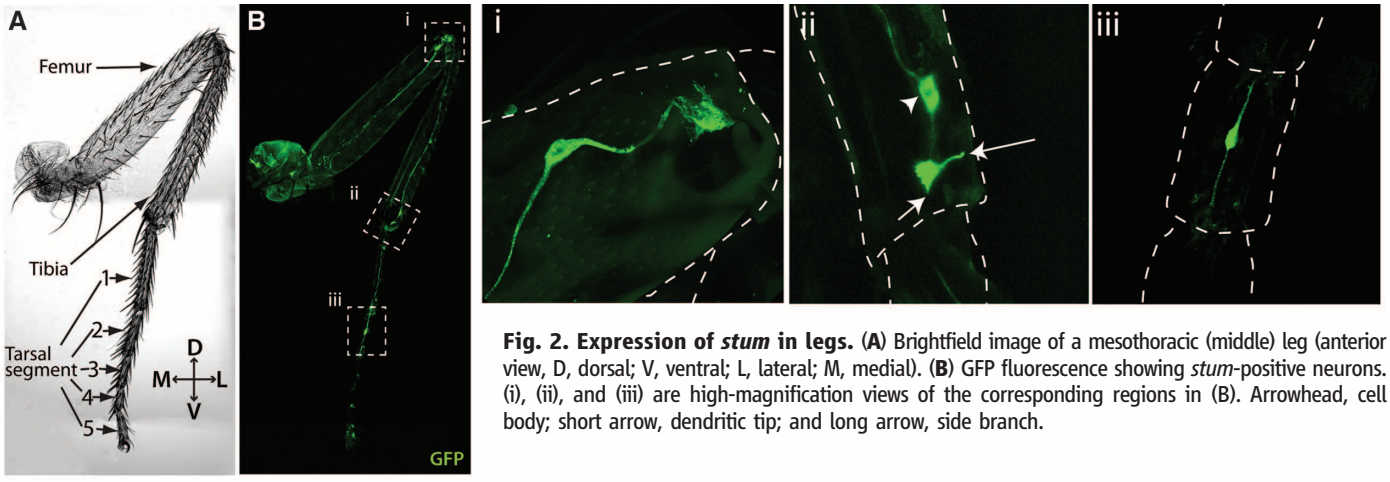

Fig. 2. Expression of *stum* in legs. (**A**) Brightfield image of a mesothoracic (middle) leg (anterior view, D, dorsal; V, ventral; L, lateral; M, medial). (**B**) GFP fluorescence showing *stum*-positive neurons. (i), (ii), and (iii) are high-magnification views of the corresponding regions in (B). Arrowhead, cell body; short arrow, dendritic tip; and long arrow, side branch.

phenotype was partially rescued (Fig. 1D), which indicated that the mutations in *stum* were underlying the uncoordination phenotype. We noted that the mouse ortholog of *stum* (National Center for Biotechnology Information, the U.S. National Institutes of Health, reference sequence: NP_001074696.1), which is only 141 amino acids long and shares 33% sequence identity with *Drosophila stum*, was also able to substantially rescue the uncoordination phenotype (Fig. 1D). Therefore, the function of *stum* appears to be conserved between distant animal species. Moreover, the rescue of the phenotype with such a short form of *stum* suggests that the C-terminal region of the fly protein constitutes the functional core.

Proprioceptive defects in adult flies have been attributed to malfunction of type I (ciliated) mechanoreceptor neurons (*4*–*6*). To test whether such defects also underlie the phenotype in the *stum* mutant, we performed electrophysiological recordings of mechanical responses from the ciliated mechanoreceptor neuron of the anterior notopleural bristle (*6*). Type I neurons of *stum* mutants were indistinguishable from controls (fig. S1). Therefore, unlike known proprioception mutants, the phenotype in *stum* mutants does not arise from a general defect in type I mechanoreceptor neurons. To identify which cells give rise to the phenotype, we used the genomic regulatory region of *stum* to drive a CD8 fused to green fluorescent protein (CD8GFP) reporter [*stum*-Gal4 driving the upstream activation sequence (UAS)–CD8GFP]. We found that *stum* expression in the legs was localized to three labeled neurons: one at the femur-tibia joint, the second at the tibia-tarsus joint, and the third spanning the second tarsal segment (Fig. 2). The cell bodies of these *stum*-expressing neurons were located near the distal end of each leg segment, and their dendrites terminated at the corresponding joints (Fig. 2).

To study whether there are *stum*-expressing cells within the ventral nerve cord (VNC), we examined it in flies that express CD8GFP using *stum*-Gal4. We found that the only fluorescent signal in the VNC originated from the axons of the leg neurons (fig. S2). The axons terminated within the neuropil that corresponds to each particular leg, branching into a bowl shape (fig. S2). This pattern is typical of neurons that take part in proprioception, such as the hair plate neurons (*7*–*9*). Therefore, the *stum*-expressing cells in the *Drosophila* body have characteristics of proprioceptive neurons that sense a property of specific joints.

We performed confocal imaging of the dendritic region of *stum*-expressing neurons and found that, close to its tip, the dendrite branches toward the lateral aspect of the joint, and this side branch terminates at a short distance from the cuticle (Fig. 2). The tips of dendrite were not associated with a cuticular structure or a scolopale. These structural features are typical features of type II (multidendritic) neurons (*10*) but are incompatible with type I mechanoreceptor neurons that terminate with a ciliary structure. Thus, *stum* uncoordination mutations affect type II mechanoreceptor neurons. Furthermore, the entire dendritic terminal of these neurons was located in a region that is devoid of musculature (fig. S3), which suggests that they do not sense the mechanical properties of muscles. Taken together, these data suggest that *stum*-expressing neurons sense a mechanical property of the joint.

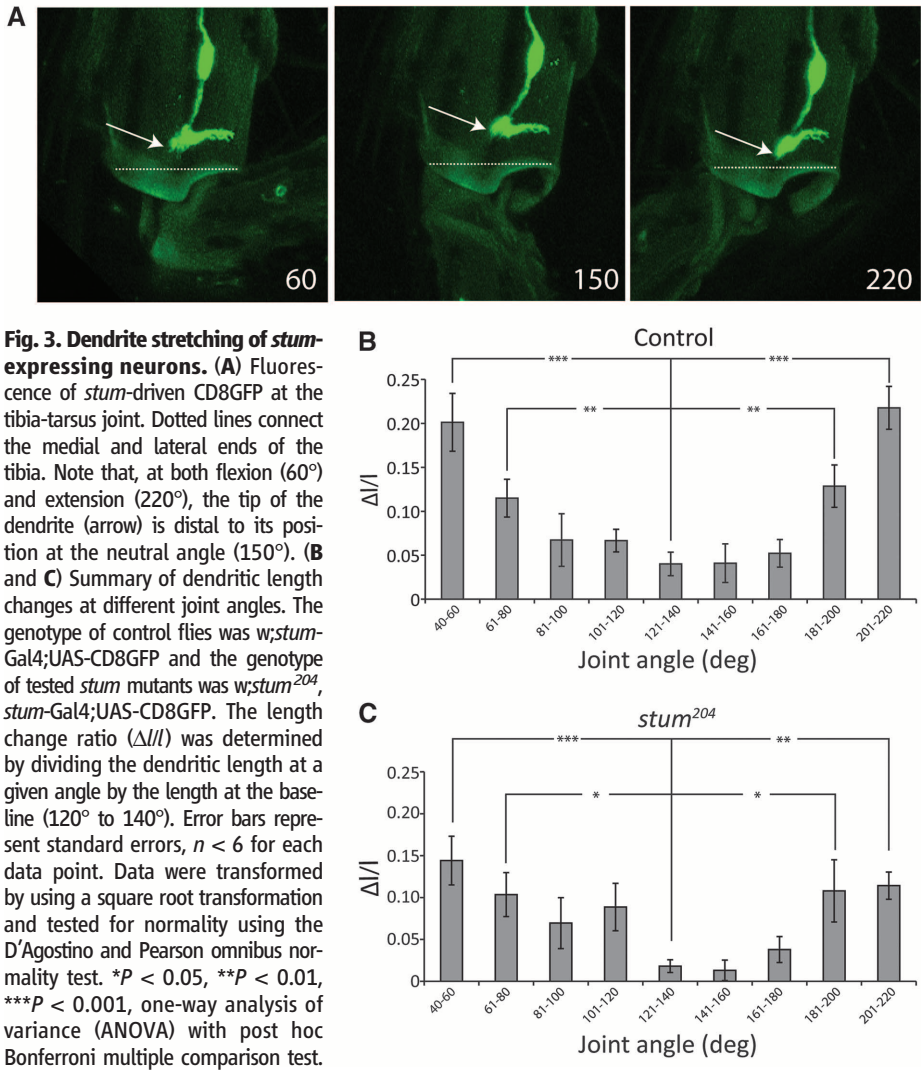

Fig. 3. Dendrite stretching of *stum*-expressing neurons. (**A**) Fluorescence of *stum*-driven CD8GFP at the tibia-tarsus joint. Dotted lines connect the medial and lateral ends of the tibia. Note that, at both flexion (60°) and extension (220°), the tip of the dendrite (arrow) is distal to its position at the neutral angle (150°). (**B** and **C**) Summary of dendritic length changes at different joint angles. The genotype of control flies was w;*stum*-Gal4;UAS-CD8GFP and the genotype of tested *stum* mutants was w;*stum*^{204}, *stum*-Gal4;UAS-CD8GFP. The length change ratio ($\Delta l/l$) was determined by dividing the dendritic length at a given angle by the length at the baseline (120° to 140°). Error bars represent standard errors, $n < 6$ for each data point. Data were transformed by using a square root transformation and tested for normality using the D'Agostino and Pearson omnibus normality test. *$P < 0.05$, **$P < 0.01$, ***$P < 0.001$, one-way analysis of variance (ANOVA) with post hoc Bonferroni multiple comparison test.

To test whether *stum*-positive neurons encode joint angles, we performed high-resolution imaging of the tibia-tarsus joint area at different angles. At each angle of the joint, we measured the total length of the sensory dendrite and its side branch. We found that the total dendrite length had a minimum typically at 130° to 170°, and it increased when the joint was shifted to either more obtuse or more acute angles (Fig. 3). These morphological changes indicate that these neurons are mechanically affected by the position of the joint. Because the tip of the side branch is stationary, it is likely that the change in total length results from the coupling of the tip of the main dendrite to the motion of the distal joint segment. The position of the dendrite and the susceptibility of its morphology to joint angle suggest that the role of *stum*-positive neurons is to sense and encode the angle of the joint.

We measured Ca^{2+} fluorescence while forcing the tibia-tarsus joint to different angles and found that the Ca^{2+} fluorescence in *stum*-expressing neurons correlated with the angle of the joint (Fig. 4). As in the morphological changes, the responses correlated with joint angle in a U-shaped manner, where both acute and obtuse angles induced increasing Ca^{2+} elevations. These results indicate that the *stum*-positive neurons encode proprioceptive information about the angle of joints. It is noteworthy that a similar U-shaped encoding of joint angles was also described in receptor neurons of mammalian joints (*11*), which suggests that sensing the deviations from a neutral joint range is universally critical for motor function.

The walking impairment in the *stum* mutant fly suggests that the gene is necessary for generating the proper proprioceptive responses in *stum*-expressing neurons. To test whether the *stum* mutations affect coupling between joint

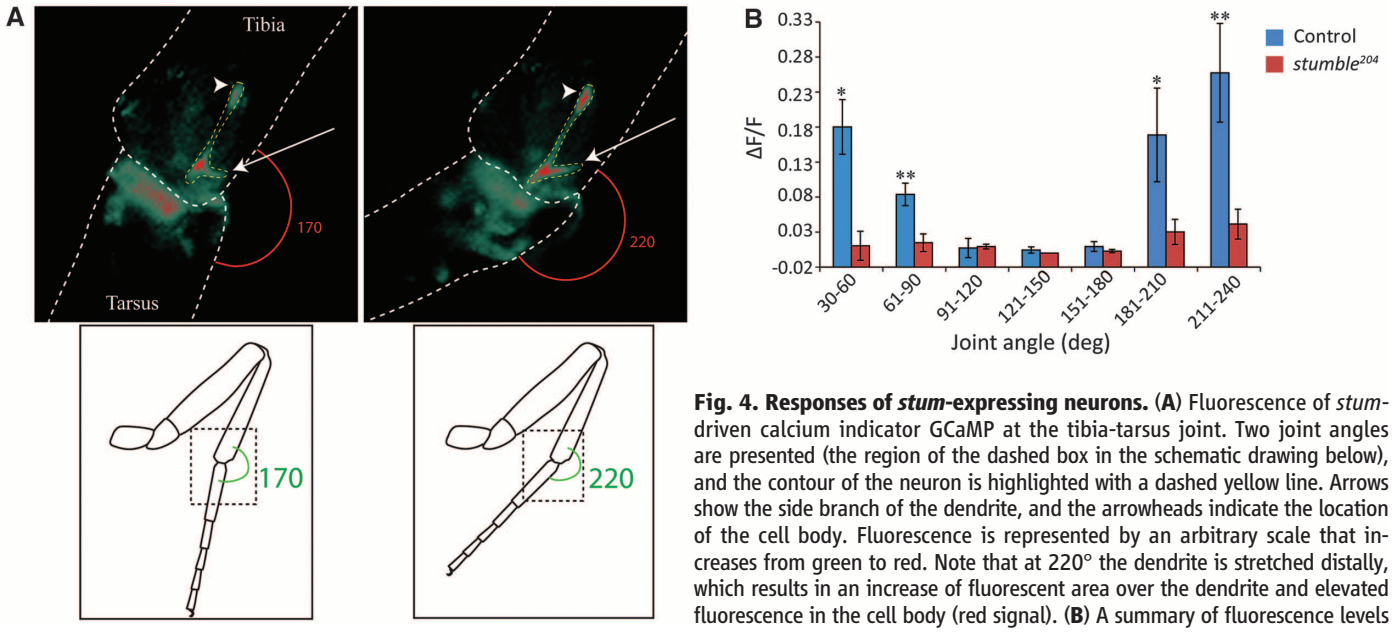

Fig. 4. Responses of *stum*-expressing neurons. (**A**) Fluorescence of *stum*-driven calcium indicator GCaMP at the tibia-tarsus joint. Two joint angles are presented (the region of the dashed box in the schematic drawing below), and the contour of the neuron is highlighted with a dashed yellow line. Arrows show the side branch of the dendrite, and the arrowheads indicate the location of the cell body. Fluorescence is represented by an arbitrary scale that increases from green to red. Note that at 220° the dendrite is stretched distally, which results in an increase of fluorescent area over the dendrite and elevated fluorescence in the cell body (red signal). (**B**) A summary of fluorescence levels of the cell body at different joint angles. The genotype of control flies was w; *stum*-Gal4;UAS-GCaMP3, and the genotype of tested *stum* mutants was w;*stum*^{204},*stum*-Gal4;UAS-GCaMP3. The $\Delta F/F$ was determined by dividing the fluorescence value at a given angle by the fluorescence at the preceding baseline (120° to 150°). Error bars represent standard errors, $n > 6$ for each data point. Baseline and response fluorescence levels were compared pairwise for each data point. *$P < 0.05$, **$P < 0.01$, Wilcoxon signed-rank test.

angles and dendritic stretching, we quantified the stretching in mutant flies that have *stum*-expressing neurons labeled with CD8GFP. We found that, in the *stum* mutant, the dendritic stretching in response to joint angles was comparable to that of control flies (Fig. 3). Thus, *stum* is not required for the mechanical coupling between joint angles and stretching of the sensory dendrites.

Although the dendritic stretching was not significantly affected in the *stum* mutant, we found that the Ca^{2+} responses to both acute and obtuse joint angles were abolished in the mutant (Fig. 4). Therefore, we conclude that *stum* is essential for transducing dendrite stretching into cellular responses.

We examined the morphology of *stum*-expressing neurons and found that, although axons (fig. S2) and cell bodies (fig. S4) of *stum* mutants were indistinguishable from controls, the sensory dendrite in mutants exhibited abnormalities (fig. S4). Most notably, in some of the *stum*-expressing neurons the tip of the dendrite was overgrown and extended into the distal segment of the joint (fig. S4). Thus, the absence of *stum* leads to a morphological defect, possibly because of the lack of mechanical responsiveness. The occasional morphological differences may account for the slight difference in the stretching profile between control and mutant dendrites (Fig. 3, B and C). The fraction of neurons demonstrating the abnormal morphology in the mutant increased from the day of eclosion to the following day (fig. S4C). As the addition of morphological changes takes place after eclosion, it is possible that *stum*-dependent activity is essential for late shape determination that can take place in adult multidendritic neurons (*12*).

We generated transgenic flies that express a GFP fused with the N terminus of Stum under UAS regulation (UAS-GFP-Stum). We found that the Stum fusion protein was specifically localized to the distal part of the sensory dendrite, although it did not accumulate substantially in any other part of the cell (fig. S5). The fluorescent signal started at the region of bifurcation and extended to both distal tips of the dendrite (fig. S5). This specific localization suggests that Stum functions in the part of the dendrite that senses stretching.

Taken together, *stum* expression in mechanosensory neurons, Stum localization to the sensory dendrite, and the abolition of responses to stretching in the *stum* mutant suggest that *stum* has an essential role in mediating mechanical sensing in receptor neurons. Because the Stum protein in most species is very small and because *Drosophila stum* is expressed in limited populations of receptor neurons, we propose that *stum* is not the mechanically activated channel. Rather, *stum* may serve as an accessory module that is essential for the proper localization or function of the transduction channels.

The stretch-receptor neurons that express *stum* present an elegant engineering solution for generating specificity to the modality of mechanical stimulus. The distal part of their dendrite bifurcates into two branches whose tips are anchored to parts of the joint that shift their relative positions. Sensing the stretching only between the two dendritic tips may tune the nerve responses to joint motions and filter out the effect of irrelevant mechanical impacts. This specificity enables the sensory neuron to relay reliable proprioceptive information to the central nervous system.

References and Notes

1. S. E. Kim, B. Coste, A. Chadha, B. Cook, A. Patapoutian, *Nature* **483**, 209–212 (2012).
2. Z. Yan *et al.*, *Nature* **493**, 221–225 (2013).
3. E. J. Koundakjian, D. M. Cowan, R. W. Hardy, A. H. Becker, *Genetics* **167**, 203–206 (2004).
4. T. Avidor-Reiss *et al.*, *Cell* **117**, 527–539 (2004).
5. M. Kernan, D. Cowan, C. Zuker, *Neuron* **12**, 1195–1206 (1994).
6. R. G. Walker, A. T. Willingham, C. S. Zuker, *Science* **287**, 2229–2234 (2000).
7. D. J. Merritt, R. K. Murphey, *J. Comp. Neurol.* **322**, 16–34 (1992).
8. R. K. Murphey, D. Possidente, G. Pollack, D. J. Merritt, *J. Comp. Neurol.* **290**, 185–200 (1989).
9. R. K. Murphey, D. R. Possidente, P. Vandervorst, A. Ghysen, *J. Neurosci.* **9**, 3209–3217 (1989).
10. R. Bodmer, Y. N. Jan, *Roux's Arch. Dev. Biol.* **196**, 69–77 (1987).
11. D. Burke, S. C. Gandevia, G. Macefield, *J. Physiol.* **402**, 347–361 (1988).
12. K. Shimono *et al.*, *Neural Dev.* **4**, 37 (2009).

Acknowledgments: We thank K. Spencer for technical assistance. The *stum* mutants were identified by screening a collection of F3 *Drosophila* lines in the laboratory of C. S. Zuker. We thank L. Stowers and T. Avidor-Reiss for kindly providing reagents. Data for this paper may be found in the supplementary materials.

Supplementary Materials

www.sciencemag.org/content/343/6176/1256/suppl/DC1
Materials and Methods
Figs. S1 to S5
References

28 October 2013; accepted 6 February 2014
10.1126/science.1247761